

**Theoretical evidence for strong correlations and incoherent metallic state in FeSe**Markus Aichhorn,<sup>1</sup> Silke Biermann,<sup>1,2</sup> Takashi Miyake,<sup>2,3,4</sup> Antoine Georges,<sup>1,2,5</sup> and Masatoshi Imada<sup>2,4,6</sup><sup>1</sup>*Centre de Physique Théorique, École Polytechnique, CNRS, 91128 Palaiseau Cedex, France*<sup>2</sup>*Japan Science and Technology Agency, CREST, Kawaguchi 332-0012, Japan*<sup>3</sup>*Research Institute for Computational Sciences, AIST, Tsukuba 305-8568, Japan*<sup>4</sup>*Japan Science and Technology Agency, TRIP, Kawaguchi 332-0012, Japan*<sup>5</sup>*Collège de France, 11 place Marcelin Berthelot, 75005 Paris, France*<sup>6</sup>*Department of Applied Physics, University of Tokyo, Bunkyo-ku, Tokyo 113-8656, Japan*

(Received 9 July 2010; published 5 August 2010)

The role of electronic Coulomb correlations in iron-based superconductors is an important open question. We provide theoretical evidence for strong correlation effects in FeSe, based on dynamical mean field calculations. Our *ab initio* spectral properties first demonstrate the existence of a lower Hubbard band. Moreover, together with significant orbital-dependent mass enhancements, we find that the normal state is a bad metal over an extended temperature range, implying a non-Fermi liquid due to formation of local moments. Predictions for angle-resolved photoemission spectroscopy are made.

DOI: [10.1103/PhysRevB.82.064504](https://doi.org/10.1103/PhysRevB.82.064504)

PACS number(s): 74.70.Xa, 71.27.+a, 74.25.Jb

**I. INTRODUCTION**

The discovery of high-temperature superconductivity in iron-based compounds triggered a tremendous amount of experimental and theoretical research. In general terms one can divide these materials into two classes. The first is based on iron-pnictogen FePn<sup>-1</sup> planes, which have to be intercalated with some spacer atoms. The second class is built up by charge-neutral iron-chalcogenide FeCn layers, where Cn can be S, Se, or Te. Superconductivity in this “11” family was first reported by Hsu *et al.*,<sup>1</sup> with a transition temperature of  $T_c \approx 8$  K for  $\alpha$ -FeSe<sub>0.85</sub>. The properties of this material can be further modified by pressure,<sup>2-4</sup> excess Fe or Se deficiencies. Another interesting route is alloying FeSe and FeTe yielding the family of FeSe<sub>x</sub>Te<sub>1-x</sub> superconductors.<sup>5</sup>

In contrast to the high-temperature superconducting cuprates, whose parent compounds are Mott insulators, the question about the strength of correlations in the iron-based superconductors is not settled. FeSe<sub>1-x</sub> has been studied with angular-integrated photoemission (PES) in Refs. 6 and 7, while angular-resolved photoemission studies (ARPES) have been performed on Fe<sub>1+x</sub>Te (Ref. 8) and FeSe<sub>x</sub>Te<sub>1-x</sub> (with  $x=0.3$  in Ref. 9 and  $x=0.42$  in Ref. 10). For all these compounds, these experiments reveal a significant iron bandwidth narrowing, by a factor in excess of  $\sim 2$ . Interestingly, recent ARPES experiments on FeSe<sub>x</sub>Te<sub>1-x</sub> with  $x=0.42$  (Ref. 10) report large mass enhancements deduced from the low-energy Fermi velocities, ranging from 6 to 23, while a smaller enhancement (in the range 2–3) was reported for Fe<sub>1+x</sub>Te.<sup>8</sup> Specific heat measurements<sup>11</sup> for FeTe<sub>0.67</sub>Se<sub>0.33</sub> gave  $\gamma = 39$  mJ/mol K<sup>2</sup>, whereas for FeSe<sub>0.88</sub> a smaller value  $\gamma = 9.17$  mJ/mol K<sup>2</sup> was reported.<sup>1</sup>

Band structure calculations based on density-functional theory (DFT) of FeSe and FeTe have shown<sup>12</sup> that the one-electron band structure of these materials is similar to the other iron-based superconductors, as regards the Fe *d* states around Fermi level. However, a recent first-principles calculation of the screened Coulomb interactions gave significantly higher values for the 11 compounds.<sup>13</sup> Dynamical

mean-field (DMFT) calculations at  $T=0$ —albeit within the iterative perturbation theory—could reproduce some aspects of the experimental results, by taking the interaction as a parameter.<sup>14</sup> Given the experimental controversies, further insight from *ab initio* theoretical predictions, in comparison with experiments, is needed in order to characterize the role of correlations for the 11 family relative to other iron superconductors (e.g., the 1111 family as LaFeAsO).

In this article, we investigate the correlation effects on the electronic structure of  $\alpha$ -FeSe in the framework of DMFT, using numerically exact Monte Carlo simulations and taking into account the full rotationally invariant Coulomb interactions, evaluated from first principles. We find that this material displays clear evidence of strong correlations. First, our results demonstrate that the satellite feature observed in PES at a binding energy of about  $-2$  eV (Refs. 6 and 7) should be interpreted as a lower Hubbard band of iron origin. Second, we find that three of the iron orbitals are characterized by a rather low quasiparticle weight, and short quasiparticle lifetimes. These features indicate deviation from conventional Fermi liquid behavior possibly associated with the formation of local moments controlled by the Hund coupling. The possible occurrence of local moments in multiband systems was discussed in a model calculation<sup>15</sup> and for 1111 pnictides<sup>16,17</sup> for parametrized interaction strengths. The situation in the 1111 is subtle. However, taking the interaction strength calculated from first principles, LaFeAsO shows moderate correlations.<sup>18</sup> Here, on the contrary, our present calculations with *ab initio* interactions strongly suggest that correlation effects are most clearly revealed in the 11 family. We make theoretical predictions for the ARPES spectrum of FeSe. Significant deviations from the DFT band structure are found, which do not simply amount to an overall bandwidth narrowing. A downward shift of the holelike bands near the  $\Gamma$ -point and an upward shift of the electronlike bands near the *M*-point are found. Although ARPES has only been reported at this stage for FeSe<sub>x</sub>Te<sub>1-x</sub>, this is consistent with the trends reported for these alloys.<sup>9,10</sup>

## II. METHODS

Our calculations use the recent implementation of the combined DFT-DMFT method in a full-potential augmented plane wave electronic-structure framework<sup>18</sup> based on the Wien2k package.<sup>19</sup> Localized Wannier-like orbitals are constructed from an energy window comprising the Fe 3*d* bands and the Se 4*p* bands, calculated in the local-density approximation (LDA). We use the tetragonal crystal structure, space group *P4/nmm*, as reported by Margadonna *et al.*,<sup>20</sup> using the experimental value for the Se position in the unit cell. A many-body self-energy, computed from DMFT using a strong-coupling continuous-time quantum Monte Carlo algorithm,<sup>21</sup> is applied to the subspace spanned by the Fe 3*d* orbitals. The matrix of Coulomb interaction parameters is calculated from first principles using the constrained random-phase approximation (cRPA),<sup>22</sup> as applied to the iron-based superconductors in Refs. 13 and 23. All screening transitions are included, except the ones within the Fe 3*d* manifold. In the notation of Refs. 13 and 23 this corresponds to the so-called *d-dp* construction. In order to avoid an orbital dependent double-counting correction, we do not use the calculated interaction matrices directly. Instead, we follow the procedure described in Ref. 18 and use the orbitally averaged Coulomb interactions. For FeSe, this yields a local Coulomb integral  $U=F_0=4.06$  eV and a Hund's coupling  $J=0.91$  eV. This is to be compared with the significantly smaller values  $U\approx 2.7$  eV,  $J\approx 0.8$  eV for LaFeAsO.<sup>13,18</sup> Please note that the definition of  $J$  is used here in terms Slater integrals, and hence differs from the definition of  $J$  in Refs. 13 and 23. We will show that the inclusion of the full rotationally invariant Hund's coupling (including spin-flip and pair-hopping) is crucial for FeSe. If not otherwise specified, all calculations were performed at a temperature  $T=290$  K using the fully localized-limit double counting.<sup>24</sup> Spectra were obtained from the imaginary-frequency Monte Carlo data using the stochastic Maximum Entropy method.<sup>25</sup>

## III. RESULTS

In Fig. 1, we compare the total momentum-integrated spectral function obtained within LDA and within DMFT. A substantial bandwidth reduction is obtained for the Fe-*d* states near the Fermi energy. Furthermore, the Se-*p* ligand states are shifted to larger binding energies as compared to LDA. In addition, there is a structure appearing at a binding energy between  $-1$  and  $-2$  eV. In order to identify the physical nature of this peak, we performed calculations for larger interactions. For computational efficiency, the calculations for varied  $U$  and  $J$  were done here with density-density interactions only. Non density-density terms affect mostly the quasiparticle states and little the LHB. It is obvious from the inset of Fig. 1 that the peak shifts toward larger binding energies with increasing  $U$ , which is the expected behavior for a lower Hubbard band (LHB), and distinguishes it from a low-energy quasiparticle excitation. The existence of a lower Hubbard band is nicely consistent with experimental PES results. Independent measurements on FeSe (Refs. 6 and 7) revealed a broad feature at a binding energy of about  $-2$  eV. It was shown in Ref. 6 that the photon-energy dependence of

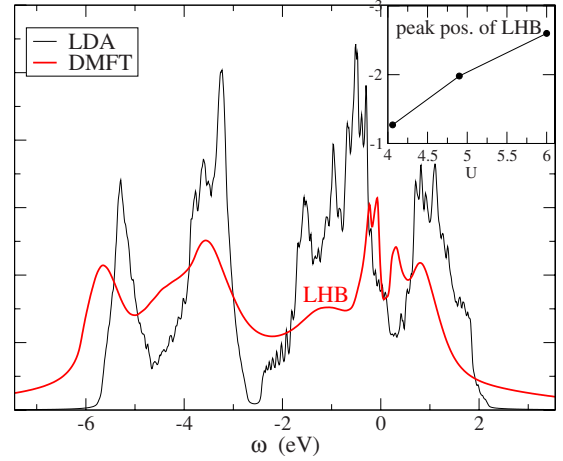


FIG. 1. (Color online) Comparison of the total LDA DOS (black, thin) to the spectral function obtained with DMFT (red, thick). “LHB” denotes the lower Hubbard band. The inset shows the evolution of the LHB as a function of  $U$ , with  $J$  scaled accordingly ( $J=0.9, 1.1, 1.3$ , respectively.)

this peak (labeled “B” in Fig. 1 of Ref. 6) indicates that it is of Fe-*d* origin. Given our theoretical results, we propose that the feature observed in Refs. 6 and 7 in this range of binding energies should be interpreted as a lower Hubbard band. To our knowledge, this is indeed the first observation of a lower Hubbard band in iron-based pnictide and chalcogenide superconductors. Indeed, the shoulder at about  $-1.5$  eV observed in PES for LaFeAsO in Ref. 26 can be explained from band theory. We also note that the position of the Se *p* bands agrees well with the experimental peak positions of  $-6$  and  $-4$  eV, corresponding to peaks “C” and “D” in Fig. 1 of Ref. 6.

Our results reveal a marked orbital dependence of the correlation effects, with significantly stronger correlations for the three orbitals  $d_{xy}$  and  $d_{xz,yz}$ , while the  $d_{z^2}$  and  $d_{x^2-y^2}$  orbitals display weaker correlations. Our conventions for the ( $x, y$ ) axis are rotated by  $45^\circ$  as compared to the crystallographic axis, so that the  $d_{xy}$  orbital in our definition is the one pointing from Fe to Se. The three orbitals displaying stronger correlations are thus the ones which form the peak of the LDA-DOS (and hence have higher weight at the Fermi level), while the two other ones display a “pseudogap” in the LDA DOS. In Fig. 2, we plot the spectral functions of each Fe *d* orbital, calculated for the same parameters as before. It is apparent that the LHB discussed above is visible mostly in the  $d_{xy}$  and  $d_{xz,yz}$  partial DOS. We have also calculated  $Z_m = (1 - \frac{\partial \Sigma}{\partial i\omega})^{-1} |_{i\omega \rightarrow 0}$ , which—in a Fermi liquid (see however below)—can be interpreted as the quasiparticle weight, and the inverse single-particle lifetime  $\text{Im} \Sigma_m(i0^+)$  of each orbital. We find that the  $d_{z^2}$  and  $d_{x^2-y^2}$  orbitals yield larger quasiparticle weights  $Z_{z^2}=0.38$ ,  $Z_{x^2-y^2}=0.47$  and longer lifetimes (corresponding to  $-\text{Im} \Sigma(i0^+)$ ) of order 0.04 eV at  $T=290$  K). In contrast, a linear fit to the slope of the self-energy for  $d_{xy,xz,yz}$  orbitals would yield lower values of the weights  $Z_{xy}=0.20$ , and  $Z_{xz,yz}=0.28$ . However, the rather short lifetimes [corresponding to  $-\text{Im} \Sigma(i0^+)_{xy} \approx 0.19$  eV and  $-\text{Im} \Sigma(i0^+)_{xz/yz} \approx 0.08$  eV] shed serious doubt on the validity of a coherent quasiparticle interpretation for those or-

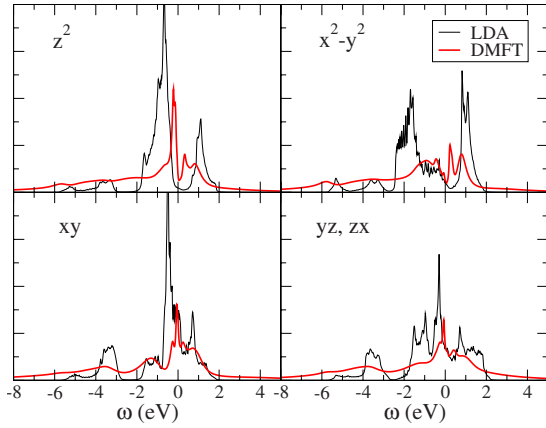


FIG. 2. (Color online) Orbital-resolved comparison of the density of states between the LDA (thin black) and DMFT (thick, red) results. The orbitals in the bottom row show strongest correlations. Note the LHB in the  $d_{xy}$  orbital.

bitals. A further decrease of the temperature from  $T=290$  K to  $T=190$  K does not reduce  $\Sigma(i0^+)$ . In order to identify coherent quasi particles the temperature has to be lower than the width of the quasiparticle, i.e.,  $T < Z \text{Im} \Sigma(i0^+)$ . Here  $Z \text{Im} \Sigma(i0^+)$  for the  $d_{xy}$  orbital corresponds to 440 K, which is higher than 290 or 190 K and, hence, no coherent quasiparticle can be expected. We checked that changing the double counting to “around-mean-field”<sup>24</sup> even increases the incoherence [ $-\text{Im} \Sigma(i0^+)_{xz,yz} \approx 0.4$ ]. We elaborate in more detail on this unconventional metallic state further at the end of this paper. The stronger degree of correlations in FeSe, compared to LaFeAsO,<sup>18</sup> manifests itself also in the partial charges of the Fe  $d$  electrons. Due to electronic correlations, the electron charge diminishes from 6.37 in LDA to 6.07 within LDA+DMFT, which should be compared to the values for LaFeAsO of 6.40 (LDA) and 6.28 (LDA+DMFT). Please note that these changes do *not* correspond to any doping effect, since the total electron count of the crystal is still integer. It is merely a redistribution of charges due to changes in the hybridization between the Fe and the ligand atoms.

We have also calculated the momentum-resolved spectral function along high-symmetry directions, displayed in Fig. 3 and compared to the LDA bandstructure. These results can be viewed as predictions for future ARPES experiments on pure FeSe. They can also be compared qualitatively with available ARPES data,<sup>9,10</sup> bearing in mind however that those actually concern the Te-substituted compound  $\text{FeSe}_x\text{Te}_{1-x}$ . The overall renormalization of the bands and the bandwidth reduction are apparent. The inverse lifetime ( $\text{Im} \Sigma$ ) increases rapidly with increasing frequency, which results in rather broad structures below  $-0.3$  eV. The DMFT quasiparticle band structure cannot be deduced from a mere rescaling of the LDA band structure. The strong orbital and energy dependence of the self-energy renormalizes the effective crystal-field splitting between the orbitals, resulting in differential shifts of the quasiparticle bands near the Fermi level. An interesting effect is seen for example near the  $\Gamma$  point. In LDA, one can see essentially only two dispersing

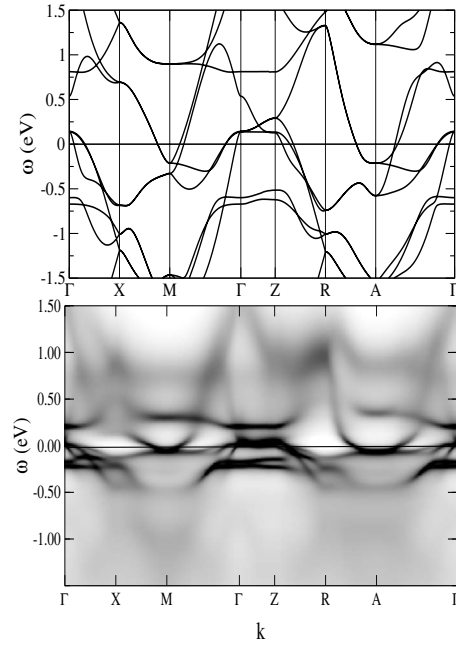


FIG. 3. Comparison of the momentum-resolved spectral function of DFT (top) to the DFT+DMFT results (bottom).

holelike bands, the outermost band being quasidegenerate. By introducing correlations, this degeneracy is lifted, and we can see three holelike excitations around the  $\Gamma$  point. This is qualitatively consistent with ARPES.<sup>10</sup> We also observe that the hole pockets near the  $\Gamma$ -point are pushed downward in energy by correlation effects, while the electronlike ones near the  $M$ -point are pushed upward, in agreement with the ARPES spectra presented in Refs. 9 and 10. The orbital character of the LDA+DMFT bands, see Fig. 4, reveals that the outermost band around  $\Gamma$  and the electron pocket around  $M$  are dominantly of  $d_{xy}$  character, which displays the largest effective mass in our calculations, see above. This is again in qualitative agreement with ARPES, where the heaviest masses were associated to the outermost hole pocket and the electron pocket. Furthermore, the broader feature at around  $-0.3$  eV is of  $d_{z^2}$  character, consistent with experiment.

Within the DMFT approach used in the present work, the effective mass enhancement of electrons in a given orbital  $m$  is related to the inverse of the weight  $Z_m$  calculated above. This suggests effective mass enhancements in the range  $\sim 2$  for the  $x^2-y^2$  orbital to  $\sim 5$  for the  $xy$  one. Direct comparison of these values to experiments is difficult in the absence of ARPES data for FeSe. ARPES measurements on  $\text{FeSe}_x\text{Te}_{1-x}$  (Refs. 9 and 10) have been interpreted as yielding very large effective masses ( $m^*/m_{\text{band}}$  between 6 and 23).<sup>10</sup> This is qualitatively consistent with the much larger specific heat coefficient reported for these alloys,<sup>11</sup> in comparison to FeSe.<sup>1</sup> It should also be kept in mind that the precise extraction of effective masses (renormalized low-energy Fermi velocities) from ARPES data by comparison to the DFT band structure is subject to rather large uncertainties, especially in view of the orbital-dependent shifts of the bands induced by correlations (see above).

Considering the full rotationally invariant Hund’s coupling<sup>16,17,27</sup> is crucial to describe properly the low-energy

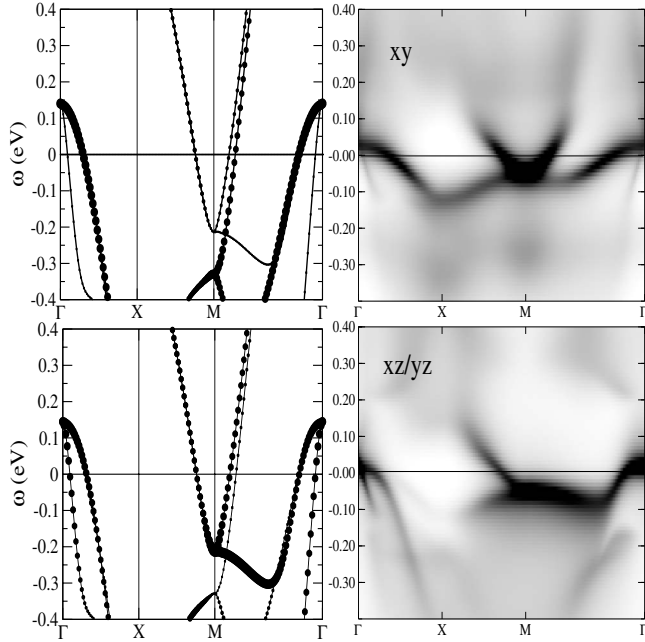


FIG. 4. Comparison of the low-energy spectral function, projected to orbital character, of DFT (left) to the DFT+DMFT results (right). Top row:  $d_{xy}$  orbital. Bottom row: degenerate  $d_{xz}$ ,  $d_{yz}$  orbitals.

physics of FeSe. Including only density-density interactions drastically suppresses the quasi-particle at low-energies (see Fig. 5), rendering the system much more incoherent for the same value of parameters, as reflected in high scattering rates  $-\text{Im} \Sigma(i\omega^+)$  in the range 0.5–1.0. In this case also, lowering the temperature (here, down to  $T=50$  K) does not reduce the scattering rates. An increase of the Coulomb parameters by even 50% does not drive the system to a Mott-insulator: at  $U=6.0$  eV,  $J=1.3$  eV there is still finite spectral weight at the Fermi level. We increased  $U$  further to  $U=10$  eV which finally leads to insulating behavior. Taken together, our results for both rotationally invariant and density-density interactions reveal that there is region of the  $(U, J)$  parameter space, where the system is in a state which is neither a Fermi-liquid, nor a Mott insulator. This region in parameter space looks similar to the selective localization found in Refs. 14 and 28, although we do not find one Mott-localized orbital, but instead three incoherent orbitals. This is also consistent with recent reports within DFT+DMFT calculations based on exact diagonalization for LaFeAsO (Ref. 17) and FeSe.<sup>29</sup>

This suggests that FeSe is just beyond the transition from the Fermi-liquid phase to an intermediate bad-metallic phase, and could be a realization of the “spin-freezing” scenario.<sup>15,16</sup> Indeed, the response to an external magnetic field increases significantly, when this phase is entered (for instance by tuning  $J$ ), which reveals the formation of localized moments. This appears to be consistent with the rather large values of the resistivity measured even on single-

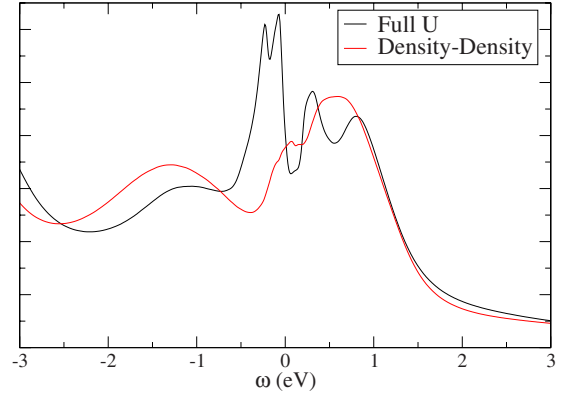


FIG. 5. (Color online) Difference of the total DOS when calculated using the full four-index  $U$ -matrix (black) and density-density interactions (red). For both calculations:  $U=4.06$  eV,  $J=0.91$  eV.

crystal samples<sup>30</sup> and with NMR (Ref. 31) and neutron scattering experiments<sup>32</sup> suggestive of strong spin fluctuations.

#### IV. CONCLUSIONS

We have presented strong theoretical and first-principles evidence for enhanced electronic correlation effects in FeSe. We have identified a Hubbard satellite in the spectral function, large orbital-dependent mass enhancements ranging from 2 to 5, and importantly large quasiparticle damping effects that may render a Fermi-liquid description of the normal state of FeSe invalid over a wide temperature range. Concerning the momentum-resolved spectral function, we find very good agreement with recent ARPES measurements. In addition to the mass enhancement, we found that a correlation induced crystal-field splitting is important to describe size and position of the hole and electron pockets at the  $\Gamma$  and M point of the Brillouin zone, respectively. As argued in Ref. 9, a simple scaling of the LDA bands is not enough to account for the measured electronic structure. The present orbital-sensitive non-Fermi-liquid behavior further indicated by their sensitivity to the Hund’s coupling may serve for understanding the interplay between the spin-charge-orbital dynamics and superconductivity in iron superconductors.

#### ACKNOWLEDGMENTS

M.A., S.B., and A.G. acknowledge discussions with V. Vildosola, L. Pourovskii, M. Ferrero, O. Parcollet, A. Liebsch, H. Ding, L. Craco, L. de’ Medici and D. van der Marel. T.M. and M.I. thank discussions with R. Arita, K. Nakamura and T. Misawa. This research was supported in part by the Agence Nationale de la Recherche under grant CORRELMAT, of IDRIS/GENCI (project 101393), the National Science Foundation under Grant No. PHY05-51164, and (MA) the Austrian Science Fund (FWF) under Grant No. J2760. The hospitality of the Kavli Institute for Theoretical Physics is gratefully acknowledged.

- <sup>1</sup>F.-C. Hsu, J.-Y. Luo, K.-W. Yeh, T.-K. Chen, T.-W. Huang, P. M. Wu, Y.-C. Lee, Y.-L. Huang, Y.-Y. Chu, D.-C. Yan, and M.-K. Wu, *Proc. Natl. Acad. Sci. U.S.A.* **105**, 14262 (2008).
- <sup>2</sup>Y. Mizuguchi, F. Tomioka, S. Tsuda, T. Yamaguchi, and Y. Takano, *Appl. Phys. Lett.* **93**, 152505 (2008).
- <sup>3</sup>G. Garbarino, A. Sow, P. Lejay, A. Sulpice, P. Toulemonde, M. Mezouar, and M. Núñez-Regueiro, *EPL* **86**, 27001 (2009).
- <sup>4</sup>S. Margadonna, Y. Takabayashi, Y. Ohishi, Y. Mizuguchi, Y. Takano, T. Kagayama, T. Nakagawa, M. Takata, and K. Prassides, *Phys. Rev. B* **80**, 064506 (2009).
- <sup>5</sup>K.-W. Yeh, T.-W. Huang, Y.-L. Huang, T.-K. Chen, F.-C. Hsu, P. M. Wu, Y.-C. Lee, Y.-Y. Chu, C.-L. Chen, J.-Y. Luo, D.-C. Yan, and M.-K. Wu, *EPL* **84**, 37002 (2008).
- <sup>6</sup>R. Yoshida, T. Wakita, H. Okazaki, Y. Mizuguchi, S. Tsuda, Y. Takano, H. Takeya, K. Hirata, T. Muro, M. Okawa, K. Ishizaka, S. Shin, H. Harima, M. Hirai, Y. Muraoka, and T. Yokoya, *J. Phys. Soc. Jpn.* **78**, 034708 (2009).
- <sup>7</sup>A. Yamasaki, S. Imada, K. Takase, T. Muro, Y. Kato, H. Kobori, A. Sugimura, N. Umeyama, H. Sato, Y. Hara, N. Miyakawa, and S. I. Ikeda, [arXiv:0902.3314](https://arxiv.org/abs/0902.3314) (unpublished).
- <sup>8</sup>Y. Xia, D. Qian, L. Wray, D. Hsieh, G. F. Chen, J. L. Luo, N. L. Wang, and M. Z. Hasan, *Phys. Rev. Lett.* **103**, 037002 (2009).
- <sup>9</sup>K. Nakayama, T. Sato, P. Richard, T. Kawahara, Y. Sekiba, T. Qian, G. F. Chen, J. L. Luo, N. L. Wang, H. Ding, and T. Takahashi, [arXiv:0907.0763](https://arxiv.org/abs/0907.0763) (unpublished).
- <sup>10</sup>A. Tamai, A. Y. Ganin, E. Rozbicki, J. Bacsá, W. Meevasana, P. D. C. King, M. Caffio, R. Schaub, S. Margadonna, K. Prassides, M. J. Rosseinsky, and F. Baumberger, *Phys. Rev. Lett.* **104**, 097002 (2010).
- <sup>11</sup>B. C. Sales, A. S. Sefat, M. A. McGuire, R. Y. Jin, D. Mandrus, and Y. Mozharivskyj, *Phys. Rev. B* **79**, 094521 (2009).
- <sup>12</sup>A. Subedi, L. Zhang, D. J. Singh, and M. H. Du, *Phys. Rev. B* **78**, 134514 (2008).
- <sup>13</sup>T. Miyake, K. Nakamura, R. Arita, and M. Imada, *J. Phys. Soc. Jpn.* **79**, 044705 (2010).
- <sup>14</sup>L. Craco, M. S. Laad, and S. Leoni, [arXiv:0910.3828](https://arxiv.org/abs/0910.3828) (unpublished).
- <sup>15</sup>P. Werner, E. Gull, M. Troyer, and A. J. Millis, *Phys. Rev. Lett.* **101**, 166405 (2008).
- <sup>16</sup>K. Haule and G. Kotliar, *New J. Phys.* **11**, 025021 (2009).
- <sup>17</sup>H. Ishida and A. Liebsch, *Phys. Rev. B* **81**, 054513 (2010).
- <sup>18</sup>M. Aichhorn, L. Pourovskii, V. Vildosola, M. Ferrero, O. Parcollet, T. Miyake, A. Georges, and S. Biermann, *Phys. Rev. B* **80**, 085101 (2009).
- <sup>19</sup>P. Blaha, K. Schwarz, G. Madsen, D. Kvasnicka, and J. Luitz, *WIEN2k, An augmented Plane Wave+Local Orbitals Program for Calculating Crystal Properties* (Techn. Universitat Wien, Austria, 2001).
- <sup>20</sup>S. Margadonna, Y. Takabayashi, M. T. McDonald, K. Kasperkiewicz, Y. Mizuguchi, Y. Takano, A. N. Fitch, E. Suard, and K. Prassides, *Chem. Commun. (Cambridge)* **2008**, 5607.
- <sup>21</sup>P. Werner, A. Comanac, L. de' Medici, M. Troyer, and A. J. Millis, *Phys. Rev. Lett.* **97**, 076405 (2006).
- <sup>22</sup>F. Aryasetiawan, M. Imada, A. Georges, G. Kotliar, S. Biermann, and A. I. Lichtenstein, *Phys. Rev. B* **70**, 195104 (2004).
- <sup>23</sup>T. Miyake, L. Pourovskii, V. Vildosola, S. Biermann, and A. Georges, *J. Phys. Soc. Jpn.* **77** Suppl. C, 99 (2008).
- <sup>24</sup>E. R. Ylvisaker, W. E. Pickett, and K. Koepf, *Phys. Rev. B* **79**, 035103 (2009).
- <sup>25</sup>K. S. D. Beach, [arXiv:cond-mat/0403055](https://arxiv.org/abs/cond-mat/0403055) (unpublished).
- <sup>26</sup>W. Malaeb, T. Yoshida, T. Kataoka, A. Fujimori, M. Kubota, K. Ono, H. Usui, K. Kuroki, R. Arita, H. Aoki, Y. Kamihara, M. Hirano, and H. Hosono, *J. Phys. Soc. Jpn.* **77**, 093714 (2008).
- <sup>27</sup>T. Pruschke and R. Bulla, *Eur. Phys. J. B* **44**, 217 (2005).
- <sup>28</sup>L. de Medici, S. R. Hassan, and M. Capone, *J. Supercond. Novel Magn.* **22**, 535 (2009).
- <sup>29</sup>A. Liebsch and H. Ishida, [arXiv:1004.2851](https://arxiv.org/abs/1004.2851) (unpublished).
- <sup>30</sup>D. Braithwaite, B. Salce, G. Lapertot, F. Bourdarot, C. Marin, D. Aoki, and M. Hanfland, *J. Phys.: Condens. Matter* **21**, 232202 (2009).
- <sup>31</sup>T. Imai, K. Ahilan, F. L. Ning, T. M. McQueen, and R. J. Cava, *Phys. Rev. Lett.* **102**, 177005 (2009).
- <sup>32</sup>M. D. Lumsden, A. D. Christianson, E. A. Goremychkin, S. E. Nagler, H. A. Mook, M. B. Stone, D. L. Abernathy, T. Guidi, G. J. MacDougall, C. de la Cruz, A. S. Sefat, M. A. McGuire, B. C. Sales, and D. Mandrus, *Nat. Phys.* **6**, 182 (2010).